Colloids and Surfaces B: Biointerfaces 113 (2014) 352–360

Contents lists available at ScienceDirect

Colloids and Surfaces B: Biointerfaces

journal homepage: www.elsevier.com/locate/colsurfb

Manufacture of layered collagen/chitosan-polycaprolactone scaffolds with biomimetic microarchitecture

Youjia Zhu [a], Ying Wan [b,*], Jun Zhang [c], Dengke Yin [b], Wenze Cheng [b]

[a] Department of Stomatology, Zhongnan Hospital, Wuhan University, 430071, PR China
[b] College of Life Science and Technology, Huazhong University of Science and Technology, Wuhan 430074, PR China
[c] Department of Chemistry and Chemical Engineering, Royal Military College of Canada, Kingston, Ontario, Canada K7K 7B4

ARTICLE INFO

Article history:
Received 6 July 2013
Received in revised form
12 September 2013
Accepted 13 September 2013
Available online 21 September 2013

Keywords:
Collagen
Chitosan-polycaprolactone copolymer
Biomimetic scaffold
Combinatorial processing technique
Articular cartilage matrix

ABSTRACT

Chitosan-polycaprolactone (CH-PCL) copolymers with various PCL percentages less than 45 wt% were synthesized. Different CH-PCLs were respectively blended with Type-II collagen at prescribed ratios to fabricate a type of layered porous scaffolds with some biomimetic features while using sodium tripolyphosphate as a crosslinker. The compositions of different layers inside scaffolds were designed in a way so that from the top layer to the bottom layer collagen content changed in a degressive trend contrary to that of chitosan. A combinatorial processing technique involving adjustable temperature gradients, collimated photothermal heating and freeze-drying was used to construct desired microstructures of scaffolds. The resultant scaffolds had highly interconnected porous layers with a layer thickness of around 1 mm and porous interface zones without visual clefts. Results obtained from SEM observations and measurements of pore parameters and swelling properties as well as mechanical examinations confirmed that graded average pore-size and porosity, gradient swelling index and oriented compressive modulus for certain scaffolds were synchronously achieved. In addition, certain evaluations of cell-scaffold constructs indicated that the achieved scaffolds were able to well support the growth of seeded chondrocytes. The optimized collagen/CH-PCL scaffolds are partially similar to articular cartilage extracellular matrix in composition, porous microarchitecture, water content and compressive mechanical properties, suggesting that they have promising potential for applications in articular cartilage repair.

1. Introduction

Articular cartilage is a type of avascular tissues and its main components include chondrocytes, Type-II collagen and proteoglycans. It is known that articular cartilage has a very limited capacity to self-repair or regenerate after degeneration or injury on account of its avascular features [1]. Current clinical therapies for articular cartilage repair usually involve micro fracturing, mosaicplasty and endoprosthetic joint replacement. However, the outcome of these clinical treatments remains unpredictable, and in particular, numerous surgical cases have not proven to be successful from a long-term point of view [2].

In search of alternative therapies, much attention for the repair of articular cartilage defects has been paid on tissue-engineering technologies [3]. To date, most approaches related to tissue engineering involve delivery of cells via porous polymer scaffolds for regeneration of tissues, and thus, the architecture of scaffolds has a decisive effect on the development of tissues in addition to chemistry of scaffolds [4]. In the case of articular cartilage tissue engineering, manufacture of scaffolds with satisfactory structures and properties has encountered specific difficulties because articular cartilage has stratiform structures and its composition and property appear to vary in an apparently anisotropic manner.

Histological examinations point out that articular cartilage has four diacritical layers, generally being named as superficial layer, intermediate layer, deep layer and calcified layer [5]. From superficial zone to calcified region, water content and Type-II collagen progressively decrease whereas proteoglycans show an inverse trend, and meanwhile, collagen fibers and chondrocytes are organized in a certain oriented manner in different layers. In addition, the diameter of Type-II collagen and compressive modulus of extracellular matrix (ECM) also change significantly from the superficial layer to the calcified layer. To date, different efforts have been made to fabricate scaffolds with certain biomimetic structures or properties approximately similar to the natural articular cartilage ECM in order to achieve improved results for articular cartilage repair. However, up to now, most studies on biomimetic scaffolds have been addressed to imitating gradient or stratified porous structures of articular cartilage ECM, and thus, they usually have limited abilities to modulate the behavior of seeded cells due to simple

* Corresponding author. Tel.: +86 27 87792147; fax: +86 27 87792234.
E-mail address: ying_x_wan@yahoo.ca (Y. Wan).

0927-7765/$ – see front matter © 2013 Elsevier B.V. All rights reserved.
http://dx.doi.org/10.1016/j.colsurfb.2013.09.028

ECM imitation [6–9]. In recent years, increasing interesting has been directed toward fabrication of more accurately biomimetic scaffolds that have preferable structures and properties more similar to that of native articular cartilage ECM [10–12]. Nevertheless, it is still far from achieving highly biomimetic scaffolds for articular cartilage repair, and engineering articular cartilage having appropriately satisfied ECM composition and properties practically similar to native articular cartilage tissue has long been a persistent challenge [6,13].

Based on compositions of articular cartilage, naturally occurring polymers such as collagen and polysaccharides have been used as preferable materials for building biomimetic scaffolds. Up to now, Type-II collagen has been widely investigated for articular cartilage repair [14]. Despite of applicability, collagen alone seems not to be competent for repairing articular cartilage lesions due to its high swelling, fast degradation and poor wet-state mechanical properties even if several types of doable crosslinkers have been utilized [15]. As one of natural polysaccharides, chitosan has also been extensively studied for applications in articular cartilage repair owing to its many advantages as well as chemical similarity to glycosaminoglycans that widely exist in articular cartilage ECM [16,17]. In spite of versatile characteristics, unmodified chitosan also shows poor wet-state mechanical properties [18] and fast degradation [19].

Chitosan-polycaprolactone (CH-PCL) is a type of grafting copolymers and has tailorable mechanical and degradation properties [19]. Polycaprolactone can be selectively grafted on the C-6 site of chitosan backbone with regulable length of side chains, which will endue the resulting CH-PCLs with a brush-like structure and enable them to be possibly soluble in aqueous medium when the PCL percentage in CH-PCLs is controlled within a proper range [20]. In view of compositions of articular cartilage ECM and merits of collagen and CH-PCLs, in the present study, an attempt was made to build a type of layered scaffolds with biomimetic microarchitecture using type-II collagen and CH-PCL as main components and sodium tripolyphosphate as a crosslinker. To endue layered scaffolds with well-controlled structures and properties, a combinatorial processing technique involving adjustable temperature gradients, photothermal heating and freeze-drying was developed. The resultant scaffolds had collagen content inversely related to chitosan content in different layers, and meanwhile, average pore-size, porosity, swelling index and compressive modulus of scaffolds altered from one layer to another in a gradient manner. These features can be synchronously achieved and they are needed for mimicking several characteristics of articular cartilage ECM.

Despite the rapidly growing variety of scaffolds, to date, clinically applicable scaffolds for articular cartilage repair are still very few [1–3,5,21]. In particular, although a variety of scaffolds and relevant techniques have become the subject of extensive enquiry, highly biomimetic scaffolds with required performance for articular cartilage repair remain poorly investigated. Therefore, relevant results for fabrications of newly devised biomimetic scaffolds together with their characterization were reported.

2. Experimental

2.1. Materials

Chitosan powder (degree of deacetylation: 90.3(±2.1)%; viscosity-average molecular weight: $3.7(\pm 0.23) \times 10^5$, measured following reported methods [22]) was supplied by Aladdin Inc. Type-II collagen, caprolactone, sodium tripolyphosphate (TPP) and hydrazine monohydrate were purchased from Sigma–Aldrich. Octane, acetic acid, Na_2HPO_4, phthalic anhydride and dimethylformamide were of analytical grade and purchased from SinoChem Ltd., China. CH-PCL copolymers were synthesized following reported methods [19,20,23].

2.2. Preparation of biomimetic collagen/CH-PCL scaffolds

A cooling circulator (CC-520w, Huber) filled with octane was used as a cooling bath. A stainless steel cylinder (150 mm in length and 50 mm in diameter) having one opened end and another end connected with a stainless steel disk (namely, sample holder) was upright set in the cooling bath in a way so that the cylinder was able to vertically move in a motor-controlled manner. In this system, the distance between the sample holder and the surface of octane was able to easily change from 5 to 100 mm and the temperature of sample holder could be effectively altered.

A circular polytetrafluoroethylene (PTFE) mold with a movable bottom was used to build scaffolds, and scaffolds were fabricated in a layer-by-layer manner. Different CH-PCLs were respectively dissolved in a 1% acetic acid solution to produce 1 wt% CH-PCL solutions. A 1.0 wt% collagen solution in 2% acetic acid was also prepared. In a typical procedure, a collagen/CH-PCL blend solution was concentrated at 50 °C and the resulting glutinous mixture was cooled down to 20 °C and added with a given amount of TPP solution. The mixture was further cooled down to 5 °C and spread onto a PTFE mold as a thin layer (around 1 mm in thickness). The mold was then moved onto the sample holder that was pre-cooled at −40 °C and was around 100 mm above the surface of octane. After the layer was solidified, surface of the layer was slightly melted using a collimated light beam generated by a parabolic reflector. The layer was then moved down (around 1 mm) together with the movable bottom of PTFE mold, and a new layer composed of collagen/CH-PCL blend gel with a prescribed weight ratio and containing the same amount of TPP was spread onto the top of the layer while moving the sample holder down 20 mm. After the new layer was nearly solidified, laminated assembly was repeated via additional layer-supraposition until required scaffold was attained. After being lyophilized at −75 °C, the resultant scaffolds were immersed first in 75% and then in 50% ethanol, and neutralized in 0.1 M Na_2HPO_4 for 30 min. After washing repeatedly with deionized water, scaffolds were freeze-dried again.

By changing composition ratio of collagen to CH-PCL in each layer and changing the processing conditions, two types of layered scaffolds with different pore parameters were built by mainly controlling the concentration of collagen/CH-PCL blend gels. One of them had similar porosity and average pore-size in each layer, and another type of scaffolds had graded pore structures changing from the top layer to the bottom layer.

2.3. Characterization

The weight percent of PCL in CH-PCL was measured using an elemental analyzer (Vario EL). Stratified scaffolds were cut into almost isopachous sheets (thickness: ca.1 mm) with the help of PTFE mold mentioned earlier. Scanning electron microscopy (SEM, XL-30 Philips) was used to view the microstructures of vertical and cross-sections of scaffolds after gold-spraying. 100 pores at 100 lattices in a SEM image for each specimen were analyzed using image analysis software and average pore-sizes were calculated by averaging these pores. Porosity of each sheet was determined using a mercury intrusion porosimeter (AutoPore IV) [19]. Swelling index (SI) of each sheet was measured via a gravimetric method. Briefly, collected sheets were immersed in PBS for 4 h, and they were then transferred into glass tubes with sintered glass filter bottom for removal of excess water via centrifugation at 2000 rpm for 2 min. SI was calculated using following equation:

$$\mathrm{SI} = \frac{W_s - W_d}{W_d} \times 100\% \quad (1)$$

where W_s and W_d are the weight of swollen sample and dry sample, respectively.

Dry scaffolds were punched into cylinders (5 mm in diameter and 4.4 mm in average thickness) with a biopsy punch. Compressive parameters were measured using a universal testing machine (Instron 5960). Load and deformation were monitored using a similar auxiliary testing unit [24], and measurements were conducted with accuracy for load down to one gram and for deformation less than 0.05 mm.

To determine mechanical parameters for different layers, cylindrical dry scaffolds (5 mm in diameter) were also cut into approximately isopachous sheets (thickness: ca.1 mm) and each sheet was measured using the same testing machine.

In the case of dry samples, they were directly compressed at a constant deformation rate of 1 mm/min. For testing hydrated samples, dry samples were immersed in PBS solution for 2 h, and absorbed water inside samples was removed using the same method described in SI measurements. Stress–strain curves of hydrated samples were measured under the same conditions applied to dry samples. Compressive modulus (E) was determined using the slope of initial linear elastic region of stress–strain curves, and the stress at 10% strain (σ_{10}) was recorded for estimating compressive strength.

2.4. Chondrocyte culture

Chondrocytes were isolated from articular cartilage of rabbit knee joints (New Zealand white rabbits, 2-week-old). The obtained articular cartilage was cut into small pieces and the resulting sample was incubated in DMEM containing 0.2% collagenase at 37 °C for 6 h or longer. The isolated cells were seeded onto cell culture flasks at a density of 10^5 cells/cm^2 in a humidified atmosphere of 5% CO_2 at 37 °C, supplementing with 10% fetal bovine serum, 50 μg/ml L-ascorbic acid, 100 U/ml penicillin and 100 μg/ml streptomycin, and replacing medium every 2 days. After around 85% confluent cells were formed, cells were detached and re-suspended in DMEM for further experiments.

Cylindrical dry scaffolds with a dimension of 5 mm in diameter and 4.4 mm in average thickness were sterilized using epoxyethane and conditioned in 75% ethanol over night. After being well prewetted in PBS, scaffolds were placed in the center of each well of 24-well culture plates for subsequent cell seeding. Chondrocytes were seeded onto scaffolds at a density of 8×10^6 cells/scaffold. After attachment for 2 h, cell-scaffold constructs were added with complete medium and cultured in a humidified incubator at 37 °C with 5% CO_2. Culture medium was changed every 2 days until harvest.

At the end of predetermined culture intervals, three cell-scaffold constructs per group were withdrawn, and each construct was horizontally sliced into four approximately isopachous sheets (around 1 mm in thickness) that corresponded to matched layer using a PTFE mold mentioned in mechanical measurements. Cell proliferation in each layer of cell-scaffold constructs was evaluated using a MTT (3-(4,5-dimethylthiazol-2-yl)-2.5-diphenyl tetrazolium bromide) essay following manufacturer's instructions. Briefly, 200 μl of serum-free medium and 20 μl of MTT solution were added to each sample, followed by incubation at 37 °C for 4 h. After vacating the supernatant, 200 μl of 10% sodium dodecyl sulfate (SDS) was added and further incubated for 8 h. Supernatant was transferred to 96-well plates and quantified for optical density at 570 nm with a microtiter plate reader against a blank SDS solution. Non-seeded sheets were used as negative control. Cell numbers were calculated using the standard curve obtained at the same time.

Some full cell-scaffold constructs cultured for a given period of time were fixed in 2.5% glutaraldehyde solution in PBS for 1 h at 4 °C. They were then vertically sectioned into thick slices, washed with PBS, stained with the nuclear stain DAPI (4,6-diamidino-2-phenylindole) and imaged via fluorescence microscopy to see the cell distribution inside the scaffolds.

Data are presented as mean ± standard deviation. Analysis of variance was performed using statistical software (SPSS 15.0 for Windows). The differences were considered to be significant at a level of $p < 0.05$.

3. Results and discussion

3.1. Fabrication of multi-layer scaffolds

In view of structure of articular cartilage ECM, we intend to fabricate multi-layer collagen/CH-PCL scaffolds having variable compositions in different layers while manipulating porous structures for each layer using adjustable temperature gradient technique. Despite certain advantages such as slow degradation and mechanical strong characteristic, PCL has several shortcomings including high hydrophobicity, lack of functional groups, neutral charge distribution and acidic degradation products [20]. Therefore, PCL content in CH-PCLs should be optimized because resultant CH-PCLs would have certain features more similar to pure PCL if weight ratio of PCL in CH-PCLs is too high. To take full advantage of both chitosan and PCL components and to consider required solubility of resultant CH-PCLs in aqueous media, four types of CH-PCLs containing PCL component at various weight percentages of 14.3, 23.2, 35.4 and 44.1 wt% and having soluble properties in aqueous media [20,23] were selected for the fabrication of collagen/CH-PCL scaffolds.

Based on many trials, a type of four-layer collagen/CH-PCL scaffolds was built and corresponding composition for each layer is shown in Fig. 1(B). Freeze-drying technique has been attracting much attention in fabrication of porous scaffolds due to its biofriendly nature and the ease of processing [12]. In the process of freeze-drying manufacture of scaffolds, pores inside scaffolds are usually generated by cryogenically removing ice crystallite formed at a fixed freezing temperature, and pore-size and porosity of scaffolds are mainly modulated by freezing temperature, freezing rate and concentration of polymer solutions. In our cases, conventional stacked freeze-processing method was found not to be as effective as expected for fabricating multi-layer scaffolds. In fact, it has been reported that in the cases of stratified scaffold construction, nonporous or oligoporous interface between two adjacent layers frequently occurs, or otherwise, two coterminous layers are often separated by crannies with diverse shapes when employing a conventional stacked freeze-processing technique, and as a result, the resultant scaffolds are usually lack of necessitated structures and properties [5,11,25].

To achieve layered collagen/CH-PCL scaffolds with designed gradient pore structures while avoiding possibly nonporous or oligoporous interface or crannies, a combinatorial processing technique involving adjustable temperature gradients, collimated photothermal heating and freeze-drying was developed because the conventional freeze-processing method was found to be unequal to this task. As described in Section 2, a PTFE mold was employed to fabricate stratified scaffolds, and it actually performs several functions: modeling the shape and size of scaffolds (see Fig. 1(A)), helping assembly of layers in a layer-supraposition manner and controlling thickness of layers. Fig. 1(B) shows a schematic representation for a four-layer scaffold in which each layer has a thickness of around 1 mm. In fact, layers inside scaffolds can be controlled more precisely so that their thickness becomes less than 1 mm because the bottom of PTFE mold can be continuously moved up or down. Noticing that the scaffold had a multifaceted structure, and collagen content decreased from 80 wt% in L1 to 20 wt%

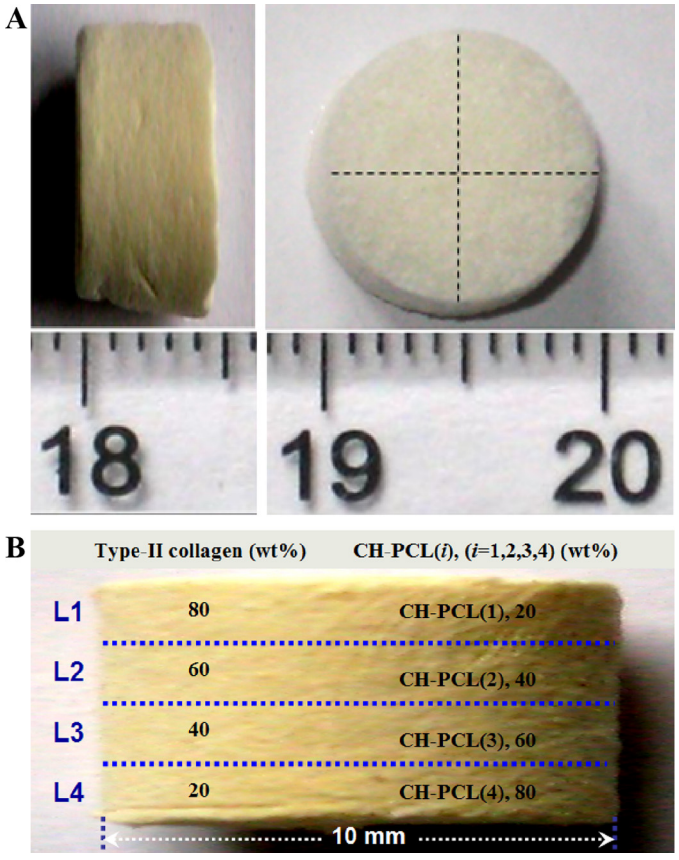

Fig. 1. Photos of a cylindrical collagen/CH-PCL scaffold (A, dotted lines denote diameter), and schematic representation of a four-layer scaffold and its composition (B, dotted lines indicate potential interface zones of layers; an equal feed ratio of TPP to matrix at 25 wt% was applied to each layer; PCL content in CH-PCL(i, i = 4,3,2,1) is 14.3(±0.98), 23.2(±1.17), 35.4(±1.26) and 44.1(±1.31) wt%, respectively; pre-cooled temperature: −40 °C, stepping descension of sample holder: 20 mm).

in L4 whereas chitosan content increased from less than 11 wt% in L1 to around 68 wt% in L4, indicating that the scaffold composition attains partial similarity when compared to articular cartilage ECM.

Besides multi-level compositions of collagen and proteoglycans, articular cartilage ECM also has an assemblage of multi-level porous structures for establishment of multiple functions. To construct gradient porous layers for layered scaffolds, regulable temperature gradients were applied to the manufacture of scaffolds, which was realized using a cooling bath together with a movable sample holder. By changing pre-cooled temperature of cooling bath or moving the sample holder, vertical temperature gradients from the bottom layer to the top layer inside scaffolds were achievable, which will potentially create multi-scale freezing compartments in different layers. Together with variable compositions and changeable concentrations of collagen/CH-PCL glutinous mixtures, microstructures of each layer could be effectively defined and controlled. With respect to photothermal heating using collimated light beam, heating was able to slightly melt the surface of each layer, which would promote formation of porous interface between two adjacent layers, and meanwhile, avoid development of crannies. In addition, heating also helped to loose the interface between the edge of each layer and the wall of PTFE mold for easy movement of layers.

In general, biodegradable scaffolds used for implantation have to endure degradation for at least several weeks with required strength. Despite presence of a certain amount of mechanically strong PCL component in each layer, scaffolds still need crosslinking to some extent considering that collagen content was high in L1, L2, and L3, and collagen has fast in vivo degradation rate. Up to now, certain types of covalent crosslinkers such as diisocyanate, epoxy compound and glutaraldehyde are frequently used to crosslink chitosan [26,27]. In the present study, TPP, a polyanion crosslinker with quick gelling capability and non-toxic property, was selected for crosslinking scaffolds because the residue of mentioned covalent crosslinkers can impair biocompatibility of the resultant scaffolds [27,28].

In principle, PCL can be grafted onto C-2, C-3 or C-6 sites of chitosan backbone. In the present instance, PCL was grafted onto the C-6 site of chitosan units by protecting amino groups at the C-2 site of chitosan backbone using phthalic anhydride as a protection reagent [19,20,23]. By doing so, amino groups at the C-2 site of chitosan units can be crosslinked by TPP. In addition, TPP can also crosslink some exposed amino groups on collagen chains via ionic interactions. In considering processing feasibility together with required properties for resultant scaffolds, the feed ratio of TPP to the collagen/CH-PCL blend gel was optimized as 25 wt%, and an equal feed ratio was applied to each layer, as illustrated in Fig. 1.

Based on photos presented in Fig. 1, it can be seen that the scaffold formed into regular cylinder with smooth surface, and the side-view in Fig. 1(A) and (B) verifies that there were no pronouncedly visual flaws that may occur during layer-supraposition assembly of scaffolds, preliminarily demonstrating that presently developed technique is practicable for fabricating multi-layer scaffolds.

3.2. Layered scaffolds with similar pore parameters

To see effect of composition and microstructures on interfaces of scaffold, an effort was made to construct a type of four-layer collagen/CH-PCL scaffolds (named as Type-I thereafter) in which each layer had various compositions as shown in Fig. 1(B) but was endued with similar porosity and average pore-size. By mainly controlling the concentration of collagen/CH-PCL glutinous mixtures while optimizing a few key processing parameters such as pro-cooled temperatures of cooling bath, distance between the sample holder and the surface of octane, and solidified time, scaffolds with desired structures were successfully built. Several representative SEM images for different interfaces in a layered scaffold are represented in Fig. 2, and dotted white lines in these images indicate interface zones.

Although there is lack of consensus regarding the optimal pore-size inside a porous polymer scaffold for cell growth and mass transport, in general, in the case of chondrocyte culture, scaffolds should have highly interconnected pores with a porosity higher than 70% while having proper pore-sizes preferentially located in a range between around 100 and 300 μm in order to facilitate cell ingrowth [29]. It can be observed from Fig. 2 that many pores with diverse shapes and various sizes were highly interconnected throughout each layer of the scaffold, and meanwhile, these pores had a relatively wider size-distribution and their size changed from several tens of microns to hundreds of microns.

Besides highly porous layers, Fig. 2 also exhibits that interface zones between adjacent layers were porous and approvingly interconnected, and there were no any typical clefts observed in the interface zones. In the present instance, porous interface zones between adjacent layers can be attributed to utilization of photothermal heating technique developed in the present study, which is proved to be successful to promote establishment of porous linkages between adjacent layers, and on the other hand, to avoid formation of cracks or clefts in the interface zones.

A set of layered scaffolds having various compositions in each layer (see Fig. 1) was assembled under the same processing conditions, and relevant parameters for their porosity, average pore-size and swelling index are plotted in Fig. 3. Data in Fig. 3 indicate that

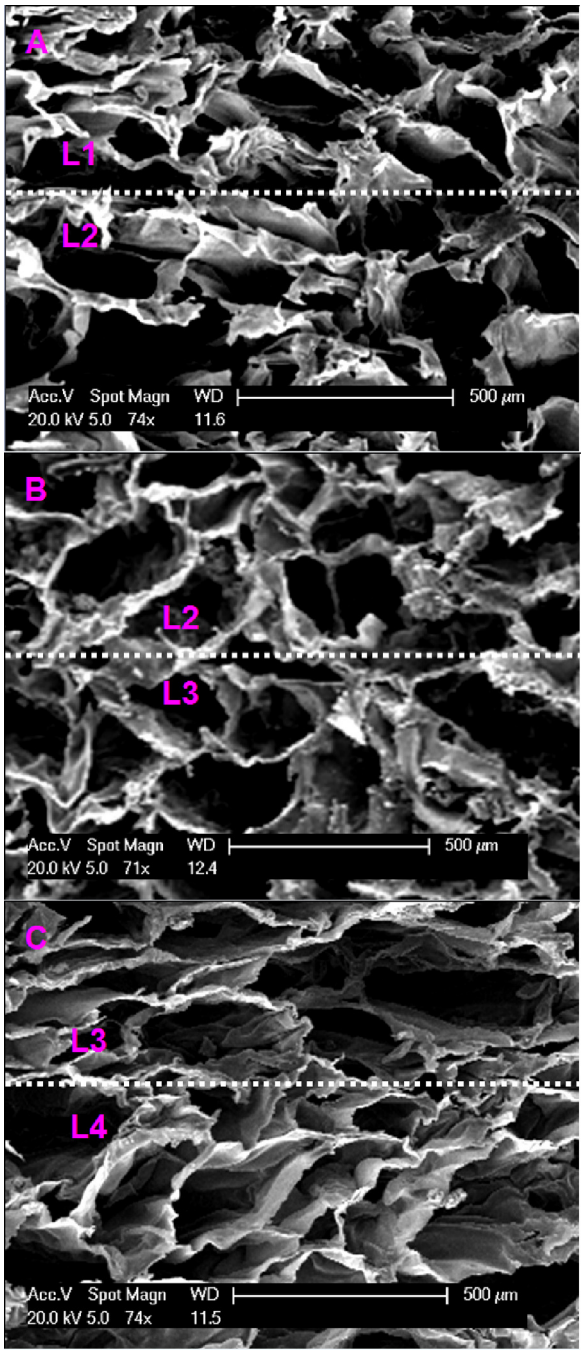

Fig. 2. Representative SEM images for interfaces inside a porous four-layer collagen/CH-PCL scaffold (Type-I).

similar average pore-size and porosity for different layers can be achieved, and compositions of layers have insignificant impacts ($p > 0.05$) on the pore parameters, meaning that in the present cases, the microarchitecture of scaffolds would be predominately regulated by processing conditions.

Fig. 3 also exhibits that there exist significant differences in swelling index for different layers ($p < 0.01$). It is known that both collagen and chitosan are hydrophilic polymers because of their polar groups, and thus, the scaffolds will swell to some extent even though a certain mount of TPP was used. Despite of nonswelling features of PCL component, the effect of PCL content on swelling index of layers would be insignificant because of low PCL content in each layer, and significant differences in swelling index should be ascribed to various degrees of crosslinking in different layers. In

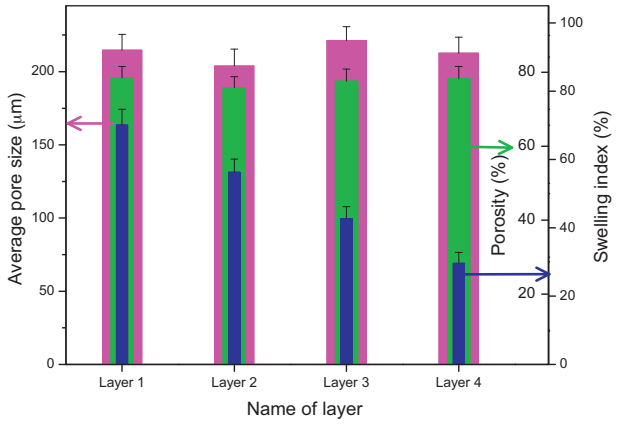

Fig. 3. Average pore-size, porosity and swelling index of some collagen/CH-PCL scaffolds (Type-I; standard deviation ($n = 4$): ±11.5 ( ), ±3.4 ( ) and ±4.4 ( )).

principle, chitosan or collagen can be crosslinked by TPP via ionic interactions between protonized $-NH_3^+$ in chitosan or collagen and negatively charged phosphate anions in TPP when an aqueous acetic acid solution is used as solvent [30]. However, the number of exposed amino groups coming from collagen chains is generally small, and the reaction rate between TPP and these exposed amino groups is low due to virgulate triple-helical structures of collagen molecules [31]. On the other hand, chitosan content was set to increase from L1 to L4. In view of these factors, cross-linking density would increase from L1 to L4, and thus, the corresponding swelling index would concomitantly decrease from L1 to L4, as shown in Fig. 3. It worth mentioning that the greater swelling index should mean higher water content for the matching layer, an thus, it can be drawn that the variation of water content in different layers in presently designed scaffolds would decrease from the top layer (matching with superficial layer) to the bottom layer (corresponding to calcified layer), which is similar to the variation tendency of water content in articular cartilage ECM [5].

3.3. Layered scaffolds with graded pore structures

It is known that besides variations of compositions in articular cartilage ECM, the porosity and pore-size also gradually change from the superficial layer to the calcified layer [5]. In our cases, it was found that three variables, i.e., concentration of collagen/CH-PCL glutinous mixtures, distance between the sample holder and the surface of octane, and solidified time of glutinous layers imposed crucial impacts on the shape of pores, average pore-size and porosity in each layer. To mimic porous microarchitecture inside articular cartilage ECM, orthogonal experimental design was applied to optimization of pore parameters for different layers inside another type of layered scaffolds (referred to as Type-II afterward) that have graded pore structures while having the same composition as elucidated in Fig. 1.

Several representative SEM images for four layers inside a Type-II scaffold are represented in Fig. 4. These images show that pores in each layer of the scaffold appear to be highly interconnected, shapes of pores randomly vary from L1 to L4, and greater pores formed more in L3 and L4 compared to L1 and L2. A series of Type-II scaffolds was measured for their average pore-size, porosity and swelling index, and collected data are presented in Fig. 5. Gradient average pore-sizes changing from around 150 to 250 μm were achieved from L1 to L4, and concomitantly, porosity increased from about 70% to 90%, revealing that presently developed processing technique is an effective one for building scaffolds with biomimetic compositions and gradient porous microarchitecture.

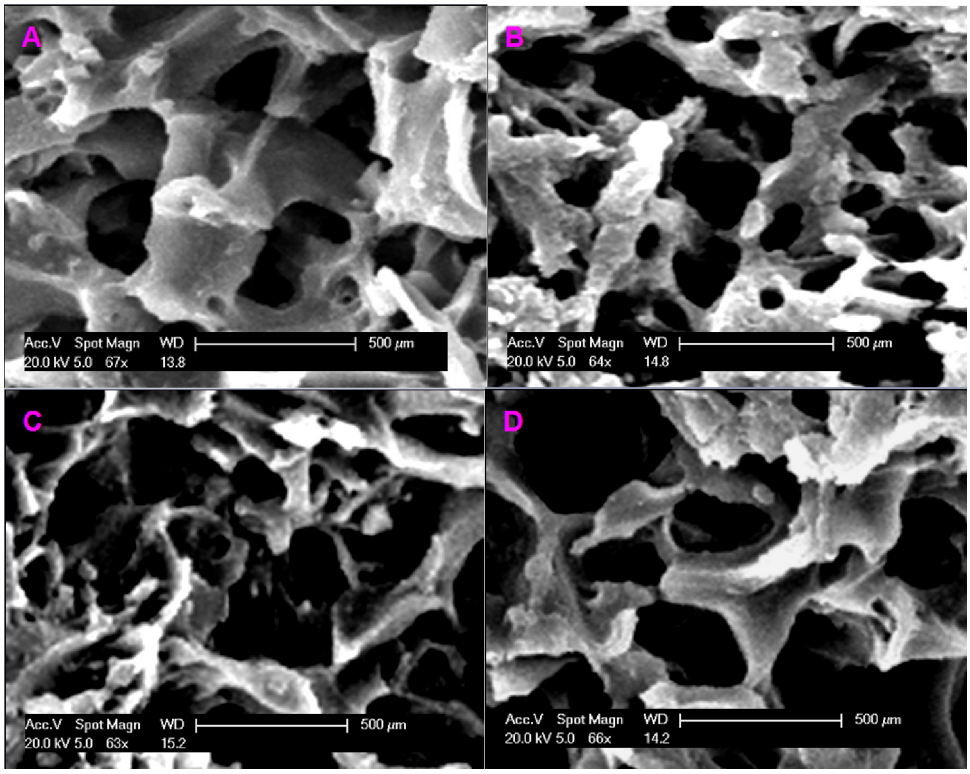

Fig. 4. Representative SEM images for four layers inside another type of porous four-layer collagen/CH-PCL scaffolds (Type-II) (A, B, C and D respectively corresponded to L1, L2, L3 and L4, as indicated in Fig. 1(B)).

It is worth noticing that swelling index for L3 and L4 in Type-II scaffolds was measurably larger when respectively comparing to the corresponding layer in Type-I scaffolds shown in Fig. 3. Larger swelling index for layers in Type-II scaffolds may be ascribed to their higher porosity and greater average pore-size, which gives rise to more easy penetration of water into scaffolds, resulting in larger swelling index. Nevertheless, swelling index for different layers in Type-II scaffolds still followed a degressive trend from L1 to L4, which indicates gradient water content in Type-II scaffolds and is in good agreement with the variation of water content inside articular cartilage ECM [5].

3.4. Compressive properties of scaffolds with graded pore structures

Compressive property of scaffolds are of particular importance in the cases of articular cartilage repair because scaffolds are frequently applied to different cartilage defects located in load-bearing zones in hip, knee and ankle, and thus, they must be able to withstand a certain pressure during implantation to help the seeded cells grow. It has been reported that compressive property of scaffolds are not only linked to shape-persistency and durability of scaffolds in practical operations but also closely correlated to modulation of cell behavior [32–34]. In the light of fact that axial compressive modulus of articular cartilage ECM increases from the superficial layer to the calcified layer, biomimetic scaffolds should also have similar mechanical characteristic. In consideration of the necessity for gradient porous microstructures, only Type-II scaffolds were selected for compressive measurements unless otherwise stated.

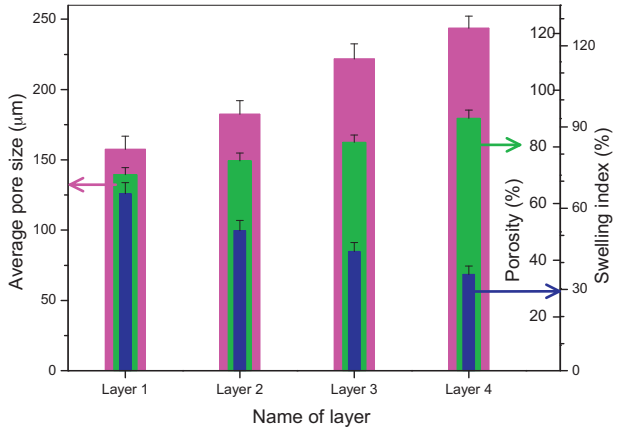

Fig. 5. Average pore-size, porosity and swelling index of collagen/CH-PCL scaffolds (Type-II; standard deviation ($n = 4$): ±10.8 ( ), ±2.9 ( ), ±4.1 ( )).

Fig. 6 shows several compressive stress–strain curves for dry and hydrated scaffold. To calculate average E and σ_{10}, a number of scaffolds were measured and relevant data are summarized in Table 1. In general, the compressive stress–strain curves for porous foams composed of non-brittle polymers exhibit a few characteristics [35,36]: linear elastic deformation at small strain, flexure deformation for the elastic materials or yielding deformation for the elasticplastic materials at relatively large strain, followed by a plateau region at apparently large strain and a solidifying region in

Table 1
Compressive mechanical parameters of dry and hydrated collagen/CH-PCL scaffolds (Type-II).[a]

Sample	Dry scaffolds		Hydrated scaffolds	
	E (MPa)	σ_{10} (MPa)	E (MPa)	σ_{10} (MPa)
L1	6.5 ± 0.49	0.59 ± 0.035	0.39 ± 0.031	0.054 ± 0.004
L2	6.9 ± 0.51	0.61 ± 0.031	0.52 ± 0.041	0.067 ± 0.005
L3	7.1 ± 0.47	0.68 ± 0.039	0.65 ± 0.033	0.097 ± 0.006
L4	7.4 ± 0.43	0.69 ± 0.044	0.74 ± 0.037	0.114 ± 0.005
Full scaffold	6.8 ± 0.49	0.63 ± 0.036	0.62 ± 0.035	0.089 ± 0.006

[a] Date in the table are presented as mean ± standard deviation ($n = 4$).

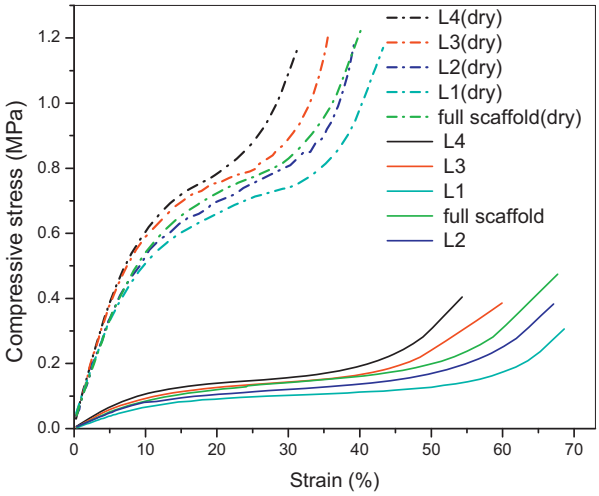

Fig. 6. Typical compression measurements for dry and hydrated collagen/CH-PCL scaffolds (Type-II, dotted curves match with dry samples and solid curves correspond to hydrated samples).

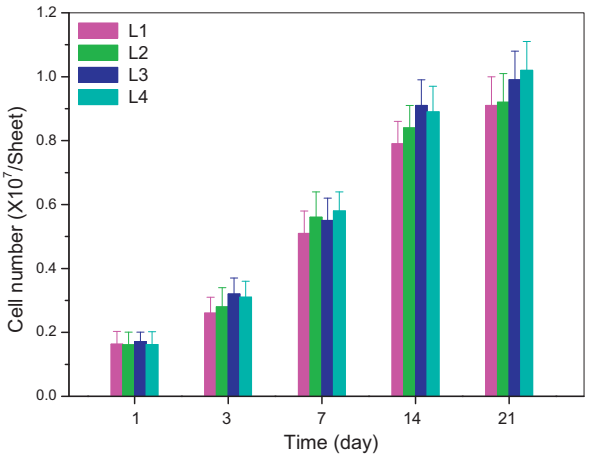

Fig. 7. Cell proliferation in collagen/CH-PCL scaffolds as measured by the MTT assay (Type-II, standard deviation ($n = 4$): ±0.09 ( ), ±0.09 ( ), ±0.08 ( ), ±0.08 ( )).

which the stress sharply increases at very large strain. All curves for dry layers and the scaffold in Fig. 6 display these four characteristics and have not shown any yielding deformation, indicating that these layers as well as the scaffold have well-defined compressive mechanical properties. In the case of dry layers, Fig. 6 shows that as layers change from L1 to L4 the plateaus zone in the matching curve gradually becomes shorter but the corresponding compressive stress does not significantly alter, suggesting that graded compositions and pore parameters have impacts on the toughness rather than the strength of layers. In general, mechanical property of porous polymer scaffolds can be correlated to various parameters of scaffolds [37,38], and in our cases, the key parameters were found to mainly include average pore-size, porosity, composition and degrees of crosslinking. As mentioned earlier, Type-II scaffolds had graded compositions and gradient pore parameters changing from L1 to L4, and meanwhile, the crosslinking of scaffolds was also heterogeneous since TPP has a limited ability to crosslink collagen molecules [30,31,39]. Although it will be extremely difficult to search out details of how these factors to regulate compressive property of layers individually, results in Fig. 6 suggested that the synergetic effect of these factors resulted in insignificant variations of E and σ_{10} for different layers in dry scaffolds ($p > 0.05$), as indicated in Table 1.

In comparison to dry layers and the scaffold presented in Fig. 6, great decreases in stress and significantly extended plateaus zones in stress–strain curves are registered for hydrated samples. These curves also indicate that as the layer changed from L1 to L4, stress of layers increased, and at the same time, the matched plateaus zone in stress–strain curves became shorter. The results for hydrated samples may be related to the ionic crosslinking characteristics of TPP. In principle, TPP is able to crosslink amino groups to some extent via ionic interactions. However, ionic linkages built by TPP molecules would become quite loose and scaffolds can notably swell when scaffolds are exposed to aqueous media because chitosan and collagen components are quite hydrophilic. Consequently, the swollen layers or scaffolds, as indicated by the swelling index in Fig. 5, would have reduced compressive strength while gaining an increased ability responded to compressive deformation, leading to great differences in stress–strain curves when compared to dry scaffolds.

In the case of hydrated samples, Table 1 reveals that E and σ_{10} vary from L1 to L4 in a significant uptrend ($p < 0.01$). Considering that under physiological conditions the implanted scaffolds will be in wet state, E and σ_{10} for hydrated samples are more significance as compared to that of dry samples. Progressively increasing trends of E and σ_{10} from L1 to L4 for hydrated layers should be attributed to the modulation of TPP. TPP is capable of crosslinking amino groups originated from chitosan more effectively than those stemmed from collagen [30,31,39], and on the other hand, chitosan content was set in an incremental manner from L1 to L4, and as a result, increasing E and σ_{10} from L1 to L4 for hydrated scaffolds were established due to differences in the degree of crosslinking for different layers. The increasing trend of E for Type-II scaffolds is a desirable property because compressive modulus of articular cartilage ECM also changes from the superficial layer to the calcified layer in a gradually increasing manner [5,6,10].

Despite relatively low compressive modulus and compressive strength of hydrated scaffolds, Table 1 shows that compressive modulus for different layers in hydrated Type-II scaffolds changed from around 0.39 and 0.74 MPa whereas full hydrated scaffolds had compressive modulus of about 0.6 MPa, and on the other hand, the lowest compressive strength of a layer in hydrated scaffolds was about 0.05 MPa. These results suggest that compressive mechanical properties of hydrated Type-II scaffolds are similar to normal human articular cartilage in knee [40,41] and also similar to many reported materials used for articular cartilage repair [42].

3.5. Proliferation and distribution of chondrocytes inside scaffolds

Type-II scaffolds were used to culture chondrocytes in vitro to assess whether the presently developed scaffolds support the growth of chondrocytes, and relevant results are presented in Fig. 7. The bar-graphs explicate that in each layer of scaffolds, the growth of chondrocytes roughly experienced three phases: fewer cells grown from day 1 to day 3; cell number notably increased from days 3 to 14; and after that, cell number slightly changed. In addition, it can also be observed that there were not significant differences in the number of proliferated cells among layers of scaffolds ($p > 0.05$). As indicated in Fig. 1(B), collagen content changed in a degressive trend contrary to that of chitosan from the top layer to the bottom layer of the scaffolds, and on the other hand, scaffolds had gradient pore structures, data shown in Fig. 7 reveal that synergetic effects arisen from composition, structure and certain properties of scaffolds result in insignificant differences in the number of proliferated cells among layers of scaffolds. Considering the initial number of seeded cells and the number of proliferated cells after culture, results in Fig. 7 confirm that these scaffolds are able to well support the growth of chondrocytes.

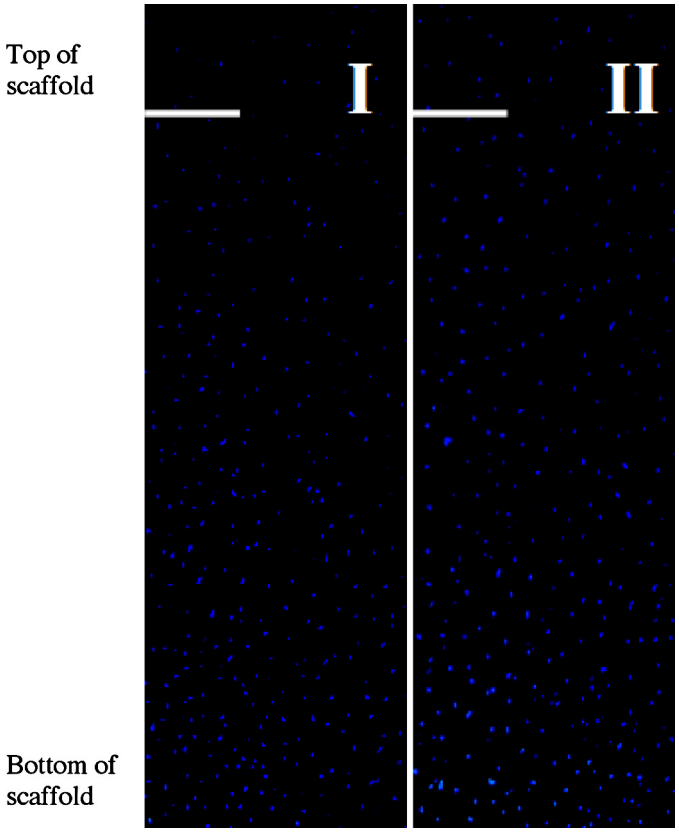

Fig. 8. Chondrocyte distribution inside collagen/CH-PCL scaffolds with fluorescence DAPI nuclei staining after culture for 2 weeks (I) and 3 weeks (II) (Type-II, scale bar: 400 μm).

To see cell distribution inside scaffolds, chondrocytes cultured in type-II scaffolds were stained with DAPI that is usually employed for staining the nucleus of fixed cells [43], and representative images taken from vertical sections in full thickness of scaffolds are shown in Fig. 8. Cells cultured for 2 weeks were randomly distributed throughout the scaffold structure without distinct blank areas or typically discontinuous zone, demonstrating that (1) scaffolds support the chondrocyte ingrowth; (2) pore-size and porosity in each layer of scaffolds are suited for the migration of chondrocytes; and (3) the interfaces between different layers inside scaffolds should be highly porous and interconnected. In addition, it can also be seen that density of cells was measurably increased after extended culture up to 3 weeks. These results suggest that presently developed processing technique enables the fabrication of scaffolds with highly interconnected porous microstructures, designed biomimetic characteristics and approving support of chondrocyte ingrowth.

4. Conclusions

The presently developed combinatorial processing technique was demonstrated to be quite practical and effective for fabrication of stratified collagen/CH-PCL scaffolds. By regulating weight ratio of collagen to chitosan for different layers in a mutually opposite manner, biomimetic compositions partially similar to articular cartilage matrix could be attained. Graded microarchitecture with highly interconnected porous layers inside scaffolds could be regulated mainly by temperature gradients and concentrations of collagen/CH-PCL glutinous mixtures. Collimated photothermal heating together with the designed mold was confirmed to be advantageous for establishment of porous interface zones without visual cracks or clefts. It was found that biomimetic compositions, graded average pore-size and porosity, gradient swelling index and oriented compressive modulus, which are just needed for mimicking certain structures and properties of articular cartilage ECM, could be synchronously achieved by using presented materials and techniques. The achieved scaffolds were able to well support the growth of chondrocytes.

Acknowledgement

This work was supported by the National Natural Science Foundation of China (Grant No. 81071470).

References

[1] E.B. Hunziker, Articular cartilage repair: basic science and clinical progress, Osteoarthritis Cartilage 10 (2002) 432–463.
[2] H. Chiang, C.C. Jiang, Repair of articular cartilage defects: review and perspectives, J. Formos. Med. Assoc. 108 (2009) 87–101.
[3] D.W. Jackson, M.J. Scheer, T.M. Simon, Cartilage substitutes: overview of basic science and treatment options, J. Am. Acad. Orthop. Surg. 9 (2001) 37–52.
[4] S. Grada, L. Kupcsika, K. Gornab, S. Gogolewskib, M. Alinia, The use of biodegradable polyurethane scaffolds for cartilage tissue engineering: potential and limitations, Biomaterials 24 (2003) 5163–5171.
[5] N.J. Castro, S.A. Hacking, L.G. Zhang, Recent progress in interfacial tissue engineering approaches for osteochondral defects, Ann. Biomed. Eng. 40 (2012) 1628–1640.
[6] F. Berthiaume, T.J. Maguire, M.L. Yarmush, Tissue engineering and regenerative medicine: history, progress, and challenges, Ann. Rev. Chem. Biomol. Eng. 2 (2011) 403–430.
[7] H. Lee, G. Kim, Cryogenically fabricated three-dimensional chitosan scaffolds with pore size-controlled structures for biomedical applications, Carbohydr. Polym. 85 (2011) 817–823.
[8] Y. Li, Y. Wang, D. Wu, K. Zhang, Q. Hu, A facile approach to construct three-dimensional oriented chitosan scaffolds with in-situ precipitation method, Carbohydr. Polym. 80 (2010) 408–412.
[9] X. Miao, D. Sun, Graded/gradient porous biomaterials, Materials 3 (2010) 26–47.
[10] N.H. Dormer, C.J. Berkland, M.S. Detamore, Emerging techniques in stratified designs and continuous gradients for tissue engineering of interfaces, Ann. Biomed. Eng. 38 (2010) 2121–2141.
[11] A. Seidi, M. Ramalingam, I. Elloumi-Hannachi, S. Ostrovidov, A. Khademhosseini, Gradient biomaterials for soft-to-hard interface tissue engineering, Acta Biomater. 7 (2011) 1441–1451.
[12] T.G. Kim, H. Shin, D.W. Lim, Biomimetic scaffolds for tissue engineering, Adv. Funct. Mater. 22 (2012) 2446–2468.
[13] M.N. Collins, C. Birkinshaw, Hyaluronic acid based scaffolds for tissue engineering—a review, Carbohydr. Polym. 92 (2013) 1262–1279.
[14] C. Chung, J.A. Burdick, Engineering cartilage tissue, Adv. Drug Deliv. Rev. 60 (2008) 243–262.
[15] T.F. LaPorta, A. Richter, N.A. Sgaglione, D.A. Grande, Clinical relevance of scaffolds for cartilage engineering, Orthop. Clin. North Am. 43 (2012) 245–254.
[16] J.K.F. Suh, H.W.T. Matthew, Application of chitosan-based polysaccharide biomaterials in cartilage tissue engineering: a review, Biomaterials 21 (2000) 2589–2598.
[17] R.A.A. Muzzarelli, Chitins and chitosans for the repair of wounded skin, nerve, cartilage and bone, Carbohydr. Polym. 76 (2009) 167–182.
[18] Y. Wan, X. Cao, S. Zhang, S. Wang, Q. Wu, Fibrous poly(chitosan-g-DL-lactic acid) scaffolds prepared via electro-wet-spinning, Acta Biomater. 4 (2008) 876–886.
[19] Y. Wan, J. Gao, J. Zhang, W. Peng, G. Qiu, Biodegradability of conducting chitosan-g-polycaprolactone/polypyrrole conduits, Polym. Degrad. Stab. 95 (2010) 1994–2002.
[20] J. Wu, C. Liao, Z. Wang, W. Cheng, N. Zhou, S. Wang, Y. Wan, Chitosan-polycaprolactone microspheres as carriers for delivering glial cell line-derived neurotrophic factor, React. Funct. Polym. 71 (2011) 925–932.
[21] G.D. Smith, G. Knutsen, J.B. Richardson, A clinical review of cartilage repair techniques, J. Bone Joint Surg. Br. 87 (2005) 445–449.
[22] Y. Wan, K.A.M. Creber, B. Peppley, V.T. Bui, Structure and ionic conductivity of a series of di-o-butyrylchitosan membranes, J. Appl. Polym. Sci. 94 (2004) 2309–2323.
[23] L. Liu, L. Chen, Y. Fang, Self-catalysis of phthaloylchitosan for graft copolymerization of ε-caprolactone with chitosan, Macromol. Rapid Commun. 27 (2006) 1988–1994.
[24] L. Shapiro, C. Smadar, Novel alginate sponges for cell culture and transplantation, Biomaterials 18 (1997) 583–590.
[25] S.C. Owen, M.S. Shoichet, Design of three-dimensional biomimetic scaffolds, J. Biomed. Mater. Res. A 94A (2010) 1321–1331.
[26] Y. Hong, H. Song, Y. Gong, Z. Mao, C. Gao, J. Shen, Covalently crosslinked chitosan hydrogel: properties of in vitro degradation and chondrocyte encapsulation, Acta Biomater. 3 (2007) 23–31.
[27] R.A.A. Muzzarelli, Genipin-crosslinked chitosan hydrogels as biomedical and pharmaceutical aids, Carbohydr. Polym. 77 (2009) 1–9.

[28] K. Park, I.C. Kwon, K. Park, Oral protein delivery: current status and future prospect, React. Funct. Polym. 71 (2011) 280–287.
[29] D. Puppi, F. Chiellini, A.M. Piras, E. Chiellini, Polymeric materials for bone and cartilage repair, Prog. Polym. Sci. 35 (2010) 403–440.
[30] Y. Luo, B. Zhang, W. Cheng, Q. Wang, Preparation, characterization and evaluation of selenite-loaded chitosan/TPP nanoparticles with or without zein coating, Carbohydr. Polym. 82 (2010) 942–951.
[31] J.A. Fallas, L.E.R. O'Leary, J.D. Hartgerink, Synthetic collagen mimics: self-assembly of homotrimers, heterotrimers and higher order structures, Chem. Soc. Rev. 39 (2010) 3510–3527.
[32] C. Chung, J.Y. Kanga, I. Yoon, H. Hwang, P. Balakrishnan, H. Cho, K. Chung, D. Kang, D. Kim, Interpenetrating polymer network (IPN) scaffolds of sodium hyaluronate and sodium alginate for chondrocyte culture, Colloids Surf. B: Biointerfaces 88 (2011) 711–716.
[33] J. Raghunath, J. Rollo, K.M. Sales, P.E. Butler, A.M. Seifalian, Biomaterials and scaffold design: key to tissue-engineering cartilage, Biotechnol. Appl. Biochem. 46 (2007) 73–84.
[34] F. Guilak, Functional tissue engineering: the role of biomechanics in reparative medicine, Ann. N.Y. Acad. Sci. 961 (2002) 193–195.
[35] Y. Wan, Q. Wu, S. Wang, S. Zhang, Z. Hu, Mechanical properties of porous polylactide/chitosan blend membranes, Macromol. Mater. Eng. 292 (2007) 598–607.
[36] B.A. Harley, A.K. Lynn, Z. Wissner-Gross, W. Bonfield, I.V. Yannas, L.J. Gibson, Design of a multiphase osteochondral scaffold. II. Fabrication of a mineralized collagen-glycosaminoglycan scaffold, J. Biomed. Mater. Res. A 92A (2010) 1066–1077.
[37] C. Tu, Q. Cai, J. Yiang, Y. Wan, J. Bei, S. Wang, The fabrication and characterization of poly(lactic acid) scaffolds for tissue engineering by improved solid-liquid phase separation, Polym. Adv. Technol. 14 (2003) 565–573.
[38] B.A. Harley, J.H. Leung, E.C.C.M. Silva, L.J. Gibson, Mechanical characterization of collagen-glycosaminoglycan scaffolds, Acta Biomater. 3 (2007) 463–474.
[39] T. Aigner, J. Stove, Collagens—major component of the physiological cartilage matrix, major target of cartilage degeneration, major tool in cartilage repair, Adv. Drug. Deliv. Rev. 55 (2003) 1569–1593.
[40] S. Treppo, H. Koepp, E.C. Quan, A.A. Cole, K.E. Kuettner, A.J. Grodzinsky, Comparison of biomechanical and biochemical properties of cartilage from human knee and ankle pairs, J. Orthop. Res. 18 (2000) 739–748.
[41] A.R. Gannon, T. Nagel, D.J. Kelly, The role of the superficial region in determining the dynamic properties of articular cartilage, Osteoarthritis Cartilage 20 (2012) 1417–1425.
[42] Q.T. Nguyen, Y. Hwang, A.C. Chen, S. Varghese, R.L. Sah, Cartilage-like mechanical properties of poly (ethylene glycol)-diacrylate hydrogels, Biomaterials 33 (2012) 6682–6690.
[43] J.M. Sobral, S.G. Caridade, R.A. Sousa, J.F. Mano, R.L. Reis, Three-dimensional plotted scaffolds with controlled pore size gradients: effect of scaffold geometry on mechanical performance and cell seeding efficiency, Acta Biomater. 7 (2011) 1009–1018.